

Enhanced Fluorescence Sensing Using Sol-Gel Materials

Brian D. MacCraith^{1,2} and Colette McDonagh¹

Received July 8, 2002; accepted July 10, 2002

The versatility of the sol-gel process with regard to the design of optimized films for fluorescence-based sensing is treated in detail. Sol-gel films are typically used to provide a microporous support matrix in which analyte-sensitive fluorophores are entrapped and into which smaller analyte species may diffuse and interact. The versatility of the process facilitates tailoring of the physicochemical film properties to optimize sensor performance. General principles of sensor optimization are presented. These include issues such as immobilization properties, refractive index control, and sensitivity enhancement. The particular advantages conferred by the use of ormosils are emphasized. In addition, the contribution made by tailored sol-gel films to recent advances in specific fluorescence-based sensor applications is emphasized. This work focuses mainly on results produced in the laboratory of the authors over the past decade.

KEY WORDS: Sol-gel; thin films; sensors; fluorescence; luminescence; ormosils.

INTRODUCTION

Fluorescence-based chemical sensors have been the focus of much research attention in recent years because of their importance in industrial, environmental, and biomedical applications [1]. This class of sensors combines the inherent sensitivity of fluorescence for chemical and biological analysis with developments in optoelectronics, which provide regular advances in component and platform technologies. The application of sol-gel materials to these sensors, especially in the form of thin films, has attracted considerable interest because of the ease of fabrication and design flexibility of the process. The nature of the sol-gel process lends itself very well to the deposition of thin films using a variety of techniques such as dip-coating, spin-coating, and spraying. In many sensor applications the sol-gel film is used to provide a microporous support matrix in which analyte-sensitive fluoro-

phores are entrapped and into which smaller analyte species may diffuse and interact [2,3]. Sol-gel films have many advantages as support matrices over polymer supports, including, for example, strong adhesion, good mechanical strength, and excellent optical transparency. The versatility of the process facilitates tailoring of the physicochemical film properties to optimize sensor performance. For example, films can be designed to have optimum porosity while minimizing leaching of the fluorophore. In this paper the versatility of the sol-gel process with regard to the design of films for specific optical sensor applications is highlighted. General principles of sensor optimization are presented. In addition, the contribution made by tailored sol-gel films to recent advances in specific fluorescence-based sensor applications is emphasized. This work focuses mainly on results produced in the laboratory of the authors over the past decade.

¹ Optical Sensors Laboratory, School of Physical Sciences, National Centre for Sensor Research, Dublin City University, Glasnevin, Dublin 9, Ireland.

² To whom correspondence should be addressed. Tel: 353-1-7005299. Fax: 353-1-7008021. e-mail: brian.maccraith@dcu.ie

SOL-GEL-DERIVED THIN FILMS

In the context of optical sensors, the sol-gel process is primarily used as a means of producing porous glass

films. The basic process involves hydrolysis and condensation polymerization of the appropriate metal (mainly silicon) alkoxide solution, followed by a temperature programme which controls the densification process [4]. The process parameters can be selected to produce a microporous glass, which can act as a support matrix for analyte-sensitive reagents, that are added to the alkoxide solution [2]. The reagent molecules, fluorophores in the context of this paper, are encapsulated in the nanometre-scale cage-like structure that grows around them, which allows smaller analyte molecules to permeate the interconnected pores.

The generic precursor solution for sol-gel-derived silica may be represented by:



where R is usually an alkyl group. The most frequently used alkoxide for silicon is tetraethoxysilane (TEOS). ROH represents the alcohol that is used as a cosolvent for the immiscible water and alkoxide. Localized hydrolysis and condensation of the alkoxide in the starting solution produces a suspension of colloidal particles (the *sol*). Polycondensation increases the connectivity between these particles so that the viscosity increases rapidly, leading eventually to a rigid network (the *gel*). This gel is a wet siloxane network that then undergoes thermal treatment (usually $<100^\circ\text{C}$) to form a dry gel (the xerogel). Xerogels are the materials of interest here because they retain the porosity that is exploited in chemical sensing. Subsequent exposure to high temperature would cause densification and eventually lead to fully densified glass.

For the production of thin films, coating takes place before gelation occurs. The precise stage in the process at which films are made is important because the viscosity of the solution increases all the time during the ageing (pregelation) period. Coatings are usually applied to substrates by dip-coating, spin-coating, or spray coating [5–7]. More recently, other techniques for film deposition have emerged, for example, screen printing and ink-jet printing [8]. For much of the work reported here, dip-coating has been used. In this case, the film thickness is determined primarily by the substrate withdrawal speed and the solution viscosity, which, in turn, is a complex function of the detailed process parameters discussed below. Spin-coating, spray coating, and screen printing are discussed in later sections of this paper.

The complex role played by the sol-gel process parameters in determining sensor film properties is illustrated by considering TEOS-based silica sol-gel films. Depending on the detailed reaction conditions, condensation may begin before hydrolysis is complete. The molar ratio of water: TEOS, henceforth called the R -value, is

an important parameter in this regard. Theoretically, $R = 2$ is sufficient for complete hydrolysis, but often the reaction does not go to completion because of the formation of intermediate species [4]. The hydrolysis that initiates the sol-gel process may be acid- or base-catalyzed. The pH value of the sol has a significant influence on the microstructural properties of the final material. The isoelectric point of silica occurs at approximately pH 2, and this value defines the boundary between so-called acid catalysis (pH <2) and base-catalysis (pH >2) [4]. Acid catalysis is associated with fast hydrolysis rates and relatively long gel times, whereas, under basic conditions, hydrolysis is slow and condensation rates are faster, giving rise to shorter gel times. Consequently, acid catalysis generally results in weakly branched structures with small pores ($<2\text{nm}$), whereas base catalysis results in a particulate gel with larger pores. Furthermore, at a given pH, an increase in the R -value causes the hydrolysis rate to increase. Such information may be used to adjust the microstructure of the final material.

The microstructure of porous sol-gel glass is dependent, however, on the complex interplay of a large number of processing parameters. Apart from R -value and pH, other important parameters that influence the microstructure include precursor type, nature of catalyst (even at a fixed pH, varying the mineral acid causes significant variation [4]), ageing time, ageing temperature, drying time, and drying temperature [4]. The structural evolution of thin films differs in many respects from that of monolithic sol-gels. In the case of films, the hydrolysis/condensation stage may overlap the deposition and drying stages. For example, as a result of rapid drying of a thin film, the gel ageing process, which enhances the porosity of monoliths, is severely inhibited.

Much of the work reported here involves sol-gel ormosil films, for which, for example, the precursor used is organically modified methyltriethoxysilane or MTEOS. These films are discussed further in a later section. The use of photo-patternable sol-gel materials as a support matrix for fluorescent sensor indicators is also reported.

IMMOBILIZATION OF FLUOROPHORES

Immobilization of the analyte-sensitive fluorophore in the porous support matrix is a critical part of the sensor fabrication process. The immobilization method chosen for a particular sensor is generally based on the following considerations:

- (1) The compatibility of the the fluorophore with the immobilization technique

- (2) Minimization of leaching, particularly for solution-based sensing
- (3) The influence of the immobilization method on the spectral or sensing properties of the fluorophore
- (4) The complexity and reproducibility of the method
- (5) Support matrix considerations; for example, the requirement of hydrophobicity or high permeability
- (6) The ease of transfer of method to mass-production.

Immobilization methods include physical entrapment, covalent binding, electrostatic binding, and adsorption. Of these, only physical entrapment and covalent binding offer sufficient stability and reproducibility for the applications discussed in this paper. Sol-gel immobilization of sensor reagents is generally achieved by addition of the reagent to the precursor solution, either at the start of the process or at a later stage before coating. In both cases, immobilization is achieved by physical entrapment in the nanometre-scale cage-like network, which grows around the dopant. Although the microporous material may be post-doped with the reagent, this will not provide efficient entrapment, which can be achieved only by adding the dopant to the precursor solution. It is immediately evident that the main feature of sol-gel entrapment is its simplicity. This, however, conceals the difficulties sometimes encountered in achieving all the desired matrix properties simultaneously because of the complex interplay between the various process parameters, as described earlier. Apart from these difficulties, sol-gel entrapment offers the advantages of a chemically inert matrix, which is both photochemically and thermally stable and has good optical transmission properties in the visible and near infrared regions.

In applications in which reagent leaching is an issue, the sol-gel process can be tailored to produce a film with reduced pore size, which results in more effective entrapment and minimal leaching, while still retaining a satisfactory sensor response. These tailoring studies are summarized in the next section. In applications in which leaching cannot be tolerated (e.g., *in-vivo* biomedical sensing), immobilization by covalent binding is an option. Here the reagent is covalently bound to the sol-gel matrix. One method of achieving this [9] is to silanize the support matrix and covalently bind the reagent via an amino group. An alternative approach used in this laboratory is to add a specially functionalized reagent complex to the precursor solution and then prepare the sol-gel film in the normal way. By functionalizing an oxygen-sensitive

ruthenium (II) polypyridyl moiety with triethoxysilane groups, a sol-gel oxygen-sensitive film, which exhibited zero leaching and a satisfactory sensor response, was produced [10].

GENERAL PRINCIPLES OF SENSOR ENHANCEMENT

Controlled Porosity and Entrapment

A key feature of sol-gel-based sensor films is the ability to control the film porosity via the process parameters. This important feature is illustrated here in the context of fluorescence-based oxygen sensing. The determination of oxygen in both gaseous and aqueous media is important in a wide range of industrial, medical, and environmental applications. The model sensor discussed here is based on a sol-gel film, in which the oxygen-sensitive ruthenium complex, ruthenium(II) tris(4,7-diphenyl-1,10-phenanthroline), or Ru(dpp)₃, is entrapped. The fluorescence emission of this complex is quenched in the presence of oxygen. The oxygen quenching process is described by the Stern-Volmer equations:

$$I_0/I = 1 + K_{SV} pO_2 \quad (2)$$

$$\tau_0/\tau = 1 + K_{SV} pO_2 \quad (3)$$

$$K_{SV} = k\tau_0 \quad (4)$$

where I and τ are, respectively, the fluorescence intensity and excited-state lifetimes of the fluorophore, the subscript 0 denotes the absence of oxygen, K_{SV} is the Stern-Volmer constant, k is the diffusion-dependent bimolecular quenching constant, and pO_2 is the oxygen partial pressure. The oxygen sensitivity is proportional to K_{SV} , which, in turn, is proportional to the oxygen permeability and diffusion coefficient of the sol-gel film [11].

A key parameter that influences oxygen sensitivity is, therefore, the film porosity. Generally, an increase in porosity (and average pore radius) is indicative of a higher diffusion coefficient in the matrix [11]. Porosity is influenced by sol-gel processing parameters, including, for example, pH, R-value (water:precursor ratio), sol ageing time, and precursor type. The role of R-value and ageing time in determining porosity, and consequently oxygen sensitivity, for TEOS sensor films is highlighted in the following example.

Figure 1 shows the fluorescence intensity as a function of gas phase oxygen concentration for TEOS-based films fabricated at (a) $R = 2$ and (b) $R = 4$. Using blue LED excitation and photodiode detection, fluorescence

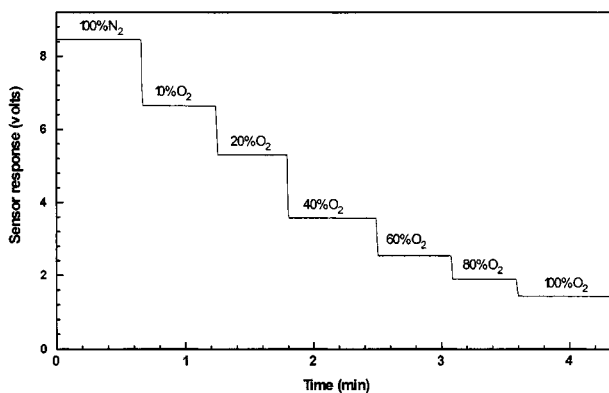
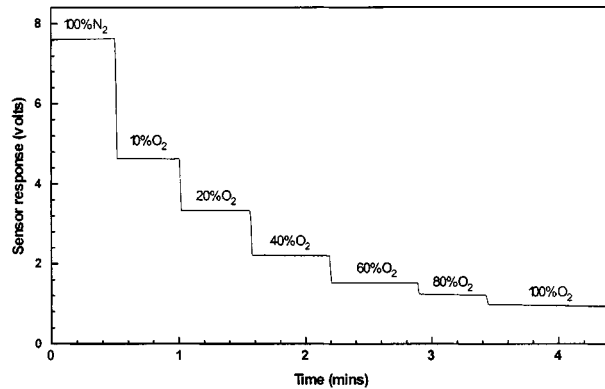


Fig. 1. Dependence of fluorescence intensity on oxygen concentration for R = 2 (top) and R = 4 (bottom) films doped with Ru(dpp)₃.

signals at a range of oxygen concentrations were obtained from sensor films incorporated in a gas flow-cell [12]. Films exhibit a non-linear dependence of fluorescence on oxygen concentration, as described by the Stern-Volmer relationship. The larger intensity drop at low oxygen concentration for R = 2 films is indicative of a higher sensitivity constant or K_{SV} for these films compared to R = 4 films. This increase in sensitivity is clear from the Stern-Volmer plots shown in Fig. 2. According to Eq. (2), a plot of I_0/I as a function of oxygen concentration has a slope of K_{SV} , the oxygen sensitivity parameter. Clearly, R = 2 films have a higher oxygen sensitivity. This is attributed to increased porosity and is corroborated by the data in Fig. 3 showing film porosity, or fractional pore volume, as a function of ageing time for both R-values. Under similar ageing conditions, the porosity is higher at the higher R-value [11]. This is consistent with faster hydrolysis and condensation rates as a result of increased water content giving rise to a denser, more cross-linked microstructure for R = 4 films. For example, the gelation times for these particular films were 170 hr

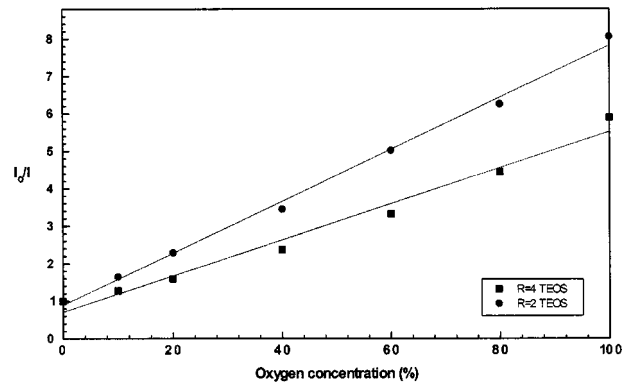


Fig. 2. Stern Volmer data extracted from Fig. 1.

for R = 2 and 12 hr for R = 4. The larger average pore size for R = 2 films compared to R = 4 is corroborated further by leaching studies performed in this laboratory using the pH-sensitive dye bromophenol blue. In this work, it was found that dye leaching rates for R = 2 TEOS films were considerably higher than for R = 4 films [13]. The role played by R-value selection in minimizing dye leaching is discussed further in the next section in the context of sensor films for dissolved oxygen.

Sol ageing, or prepolymerization, is a process whereby the sol is allowed to stand, either at room temperature or at an elevated temperature, for a period, during which hydrolysis and condensation reactions cause aggregation and cross-linking. The process can enhance the porosity of the films, as seen in Fig. 3, as well as allow the sol to attain a viscosity sufficient for the particular coating process. For both R = 2 and R = 4 films, oxygen sensitivity increases with ageing time.

It is also evident from Fig. 1 that the choice of R-value in the fabrication process can be used to tailor the

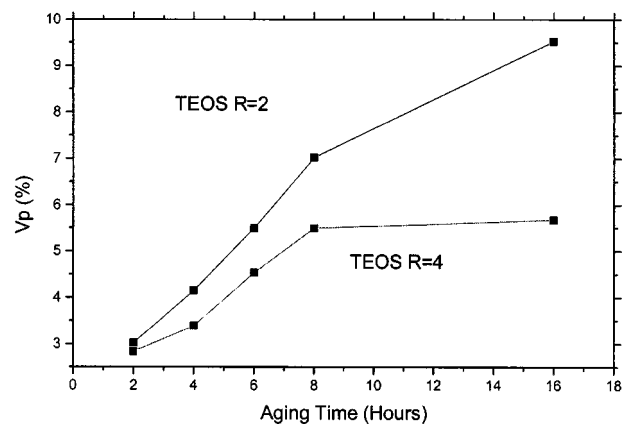


Fig. 3. Porosity as a function of ageing time for TEOS R = 2 and R = 4 films.

quenching response for a particular oxygen concentration range. For example, the response at low oxygen concentrations can be optimized by choosing $R = 2$, whereas films produced with $R = 4$ films give a more gradual response over a wider concentration range. The authors have investigated R -values between 2 and 6, and the uniformity of sensitivity over the full concentration range has been shown to increase with R -value over this range.

Organic Modification

Although TEOS-based films display excellent oxygen-sensing characteristics in the gas phase, this is not the case for dissolved oxygen sensing. TEOS films exhibit substantially reduced oxygen sensitivity in the aqueous phase compared with gas phase behavior [11]. This is attributed mainly to the hydrophilic nature of the film surface, which derives from a high surface coverage of hydroxyl groups. Oxygen has both a relatively low solubility and diffusion coefficient [14] in water. This results in a low dissolved oxygen sensitivity for hydrophilic films where the oxygen accesses the fluorophore via the water contained in the pores. For this application, using sol-gel organically modified silica (ormosil) films considerably enhances the sensitivity.

In ormosil films, the Si–OH groups on the material surface are replaced by Si–R groups, where R is typically a methyl or ethyl group [15,16]. These groups have a poor affinity for water and they render the surface hydrophobic. A hydrophobic film surface enhances the dissolved oxygen quenching process by reducing water solubility in the matrix and causing the partitioning of oxygen out of solution into the gas phase within the sensing film. Hydrophobic sol-gel films are fabricated by using an organically modified precursor such as methyltriethoxysilane (MTEOS) or ethyltriethoxysilane (ETEOS). A systematic study was carried out to investigate the influence of film hydrophobicity on oxygen sensitivity. Figure 4 shows Stern-Volmer plots for four films fabricated with different MTEOS/TEOS ratios. The curvature of these plots is attributed mainly to the heterogeneity of the fluorophore environments in the sol-gel films [12]. Clearly, the pure MTEOS film has the largest sensitivity, corresponding to the largest Stern-Volmer value. These values are obtained from the linear part of the plot, above ~ 5 ppm oxygen concentration.

By analogy with the R -value tailoring of the oxygen sensitivity of TEOS films in gas phase discussed earlier, the sensitivity of MTEOS films also can be tailored for both gas-phase and DO sensing [12]. In addition, it has been shown that dye leaching in aqueous phase is almost eliminated for films fabricated at $R = 4$. This is consistent

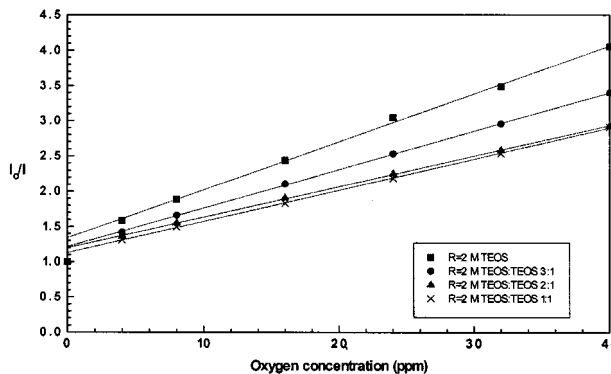


Fig. 4. Stern-Volmer plots of dissolved oxygen (DO) sensitivity for a range of films fabricated from different MTEOS/TEOS mixtures.

with results for TEOS reported in the previous section, whereby the higher R -value promotes faster hydrolysis and condensation rates, which results in a denser microstructure and better dye entrapment.

Recent work [11] has shown that, as well as being able to tailor the oxygen diffusion coefficient via the porosity of the film, the oxygen solubility also can be tailored. The bimolecular quenching constant, k , in Eq. (4) is related to both the diffusion coefficient and the solubility. For a given matrix, the diffusion coefficient, and hence the oxygen sensitivity, can be adjusted by controlling the porosity, as discussed previously. The solubility, which obeys Henry's Law at low pressures, is generally regarded as a constant for a particular support matrix [17]. A range of TEOS and MTEOS films was investigated and Stern-Volmer constants and oxygen diffusion coefficients were evaluated independently. The results are summarized in Table I, in which data from the literature on some widely used polymer-based oxygen sensor films are included for comparison purposes [18–20]. The TEOS and MTEOS films were chosen to have similar Stern-Volmer constants. Diffusion coefficients were measured by modeling the sensor response time [21], and decay times were measured using a laser system. The solubility was evaluated from these data using an estimate for the bimolecular quenching constant from Liu

Table I. Stern-Volmer Coefficients, Unquenched Decay Time, Diffusion Coefficient, and Solubility Data for Sol-Gel and Polymer Films

Film	K_{SV} (Pa) ⁻¹	τ_0 (μ s)	D (cm ² /s)	S (Pa) ⁻¹
TEOS $R = 4$	3.50×10^{-5}	5.1	3.5×10^{-9}	5.8×10^{-4}
MTEOS $R = 2$	3.24×10^{-5}	4.9	7.8×10^{-8}	2.5×10^{-5}
Silicone RTV 118	2.5×10^{-4}	5.3	12×10^{-6}	1.2×10^{-6}
Polystyrene	7.0×10^{-6}	5.3	1.87×10^{-7}	2×10^{-6}

et al. [22]. It is clear from the table that not only is there a difference in solubility between TEOS and MTEOS films but also that these values are quite different from those of typical polymer films. It is suggested that the order of magnitude increase in solubility for sol-gel films compared with polymer films arises from the relatively rigid nature of the sol-gel structure characterized by a large number of micropores, resulting in a large free volume. The intermediate value for MTEOS is consistent with the hybrid nature of the ormosil film, in which the structure is less rigid and more polymer-like, but with more free volume than a typical polymer film. Not only does this increased oxygen solubility for sol-gel films enhance the overall oxygen sensitivity, but this study also shows that solubility is yet another parameter that can be tailored in the sol-gel process.

Sensor response times were measured for the films discussed above by incorporating the sensor in a fast solenoid valve so that gas concentrations could be changed rapidly and the influence of gas exchange lines minimized [23]. The corresponding diffusion coefficients were calculated using a published theoretical model that describes the response and recovery behavior of such films [21]. Our measurements and calculations showed that, for a given thickness and similar processing conditions, MTEOS films exhibit a considerably shorter response time and a larger value of diffusion coefficient than do TEOS films. The diffusion coefficient data are presented in Table I. The smaller diffusion coefficient for TEOS may be due to a complex diffusion process arising from the high concentration of adsorbed water on the hydrophilic pore surface. The diffusion process may involve oxygen continuously partitioning into and out of the water layer, thereby giving rise to slower diffusion. This study illustrates that the choice of precursor plays an important role in tailoring the diffusion coefficient, as well as the porosity, as discussed earlier.

Refractive Index Control

Many optical sensors, both absorption and fluorescence based, use waveguiding principles. Many optical fibre-based evanescent-wave sensors employ a thin, porous sol-gel film that has been coated on a length of de-clad optical fibre and that is doped with an analyte-sensitive reagent. For fluorescence-based sensors, the fluorophore is excited evanescently in the sol-gel film and the analyte-dependent fluorescence is coupled back into the fibre core and guided to the detector [24]. The quantity of evanescent power that can interact with the fluorophore is critically dependent on the refractive indices of the fibre core and sol-gel cladding. Hence, the ability to tailor

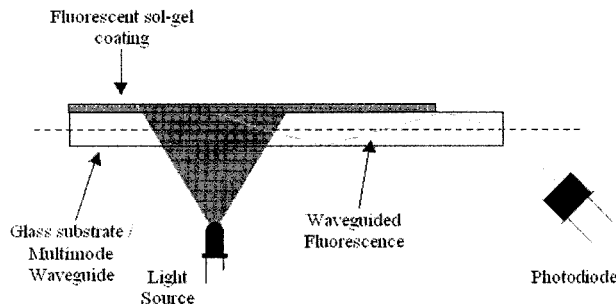


Fig. 5. Edge detection configuration for planar fluorescence sensor.

the sol-gel refractive index is crucial to optimizing sensor performance. Typically, a porous silica sol-gel film has a refractive index ~ 1.43 , but this value can be adjusted by choice of process parameters such as sol pH, ageing time, and, in particular, the sol-gel precursor.

The importance of refractive index control is illustrated well by a novel fluorescence-sensing platform based on a dye-doped, porous sol-gel film coated on a planar glass substrate [25]. A schematic diagram of the sensor is shown in Fig. 5. The fluorescent sol-gel coating is illuminated directly by an LED, in contrast to the evanescent-wave excitation normally employed in such systems. A large proportion of the resultant fluorescence couples into the substrate and is guided to a detector at the end-face of the substrate. Theoretical studies [26] have shown that the light exiting the end-face is highly anisotropic and that the optimum angle of detection is related to the relative refractive indices of the sensor film and substrate. This is shown in Fig. 6, where the angular emission patterns from doped sol-gel films of varying refractive indices, obtained by mixing silica and titania precursors, are compared. [Note: The substrate refractive index the relevant wavelength region is 1.515]. It is clear from this figure that both the angle of maximum wavegu-

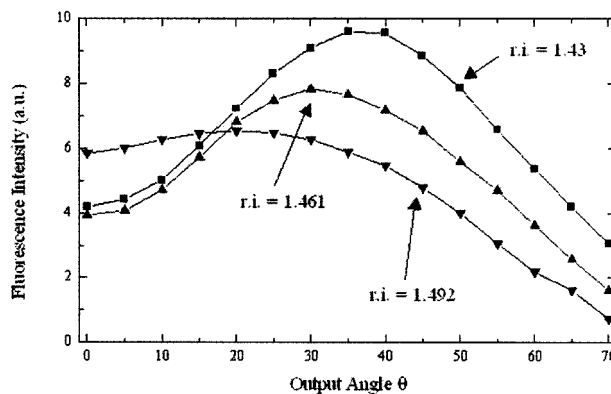


Fig. 6. Angular dependence of edge-detected fluorescence signal for a range of film refractive index values.

ide emission and the maximum intensity increase with decreasing refractive index of the sensor film within the range examined. More importantly, the intensity maximum becomes sharper as the film index decreases, and this well-defined maximum facilitates the spatial separation of fluorescence and excitation light, thereby eliminating the need for optical filters. The sensor optimization principles that are applied to this generic sensing platform are facilitated significantly by the flexibility of sol-gel processing and, in particular, by the ease with which refractive index can be adjusted.

SPECIFIC EXAMPLES OF SENSOR APPLICATIONS

In the previous section, the general principles of sol-gel material design for sensor optimization were presented. In this section of the paper, the ability to exploit these principles is treated in greater detail by highlighting specific examples of recent sensor applications.

Hybrid Sol-Gel Films for Carbon Dioxide Sensing

Optical carbon dioxide (CO₂) sensors are becoming increasingly important for many applications. An important application is the detection of CO₂ in modified atmosphere packaging (MAP) food packages. Food products are often packed under a protective atmosphere of nitrogen or CO₂ with a very small residual oxygen concentration. Carbon dioxide is typically used to decrease bacterial growth rates [27]. Because package integrity is an essential requirement for the quality of MAP food, leakage detection is a very important part of MAP technology. Currently, MAP food packages are mostly sampled destructively, whereby a sample of the gas atmosphere within the package is extracted and analyzed remotely by infrared analysis for CO₂ content. A desirable alternative is the printing of a fluorescent sensor strip inside the package thereby this can be optically scanned to monitor gas concentration. Two critical requirements for this strip are (1) sensitivity over the full range (0–100%) of CO₂ concentration and (2) ease of printing on the plastic packaging. Sol-gel-based films satisfying both of these criteria have been developed. Only the sensing issue is addressed here.

Two different approaches to fluorescence-based CO₂ sensing that exploit sol-gel-derived materials are described here. The first approach employs a fluorescence resonance energy transfer (FRET) technique using phase fluorimetric detection [28]. Here the CO₂-dependent rate of energy transfer, between a donor ruthenium complex

and a pH-sensitive dye (the acceptor), is monitored by measuring the fluorescence decay time. In the second approach, a dual luminophore referencing (DLR) technique [29,30] is employed, whereby a pH-dependent fluorescence intensity is converted to a CO₂-sensitive phase shift. Both approaches employ a porous, hydrophobic MTEOS ormosil matrix to entrap the sensing indicators and these films. Detection in the time domain, which has many advantages over conventional intensity-based sensing, is exploited in both cases. The techniques of phase fluorimetry and DLR have been described elsewhere [29,31,32] and will not be dealt with in great detail here.

Fluorescence Resonance Energy Transfer (FRET) Membranes

Absorption-based CO₂ sensors involve the water-mediated protonation by CO₂ of an anionic pH indicator dye. The principle of FRET involves the conversion of this CO₂-dependent absorbance to a fluorescence signal. A long-lifetime luminescent donor is co-doped with a pH-sensitive acceptor. The spectral overlap between the donor emission band and the absorption band of the acceptor, coupled with the spatial proximity of both indicators, facilitates energy transfer whereby the donor fluorescence and lifetime are a function of the CO₂ partial pressure. The donor indicator selected for this work was Ru(dpp)₃, the same indicator used previously for oxygen sensing. This indicator is well matched spectrally to the pH indicator Sudan III. Both indicators were entrapped in a hybrid sol-gel/polymer matrix. The predominantly MTEOS-based matrix, with a small ethyl cellulose component, enables the sensor to retain the superior chemical and mechanical stability of the sol-gel material while achieving the maximum sensitivity afforded by the polymer component. The pH indicator was reacted with the base tetraoctylammonium hydroxide (TOA–OH) to form a hydrated ion-pair [28]. The lipophilic base stabilizes the deprotonated form of the indicator in the matrix and provides the sensing chemistry with the necessary water of crystallization. The amount of added base was tailored to ensure adequate sensitivity over the complete range of CO₂ concentration, as required for the MAP application. These hybrid membranes were found to exhibit superior performance when compared to pure polymer-based FRET membranes [28]. The signal-to-noise ratio (SNR) of sol-gel-based CO₂ membranes was greatly increased compared to the behavior for the more flexible polymer structure, as the rigid sol-gel cage structure minimizes vibrational deactivation of the ruthenium complex. Apart from better dynamic range and SNR, the sol-gel films

are mechanically more robust and have superior optical transmission properties than their pure polymer counterparts. A typical response to CO_2 is shown in Fig. 7. Clearly, the film exhibits good repeatability and high SNR, but the most important feature is the extended operational range from 0 to 100% CO_2 , which is not typical of CO_2 fluorescence-based sensors.

Dual Luminophore Referencing (DLR) Membranes

Most reported fluorescence-based CO_2 sensors rely on the intensity change of a fluorescent pH indicator such as 1-hydroxypyrene-3,6,8-trisulfonate (HPTS). These are mainly intensity-based sensors because the short lifetime (~ 3 ns) of HPTS does not easily facilitate the more desirable time domain detection method. Recently, a novel sensing scheme has been introduced that offers the possibility of overcoming some of the problems normally associated with fluorescence intensity-based sensors [32]. Dual luminophore referencing (DLR) is an internal ratiometric method whereby an analyte-sensitive fluorescence intensity signal is converted into the time domain by co-immobilizing an inert long-lifetime reference luminophore with similar spectral characteristics [33,34]. Using a phase-fluorimetric approach, the composite phase signal arising from the two luminophores provides an intensity-referenced output in the time domain. (See ref. [29] and [30] for greater detail on this important technique). Excitation and emission wavelengths of ruthenium complexes and HPTS are sufficiently matched to make them excellent candidates for a DLR-type CO_2 sensor. In this work, because the ruthenium complex is used as a reference luminophore, its oxygen sensitivity can pose a significant problem. Entrapping the reference

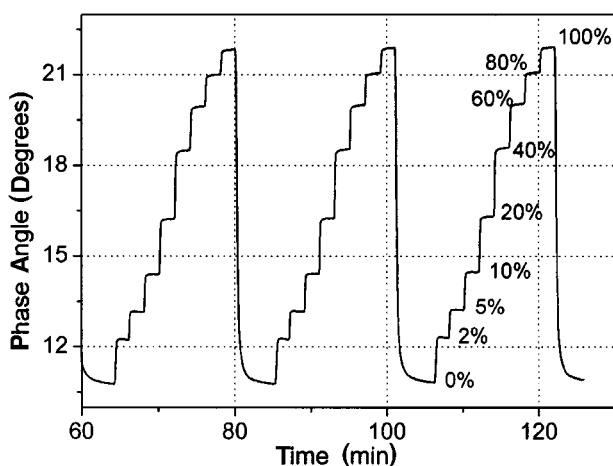


Fig. 7. Calibration plot for FRET-based CO_2 sensor.

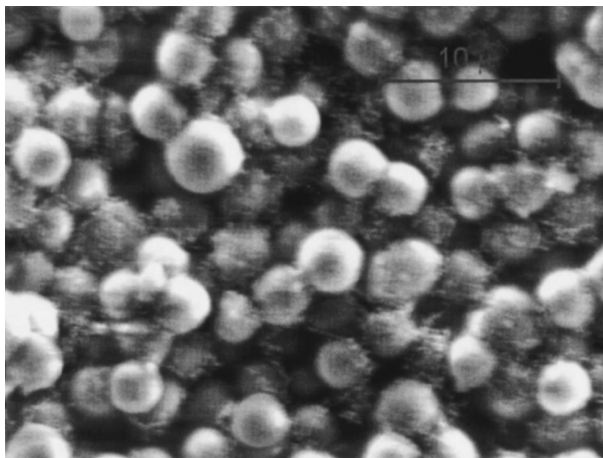


Fig. 8. Microscope photograph of TEOS-derived microparticles doped with ruthenium complex.

ruthenium complex in dense sol-gel TEOS microparticles, shown in Fig. 8, has surmounted this difficulty. The HPTS and the sol-gel reference particles have been co-immobilized in an ormosil MTEOS matrix. A hydrophobic ormosil material is selected to minimize the influence of ambient humidity on the water-mediated sensing chemistry. As in the case of the FRET-based CO_2 sensor, the sol-gel ormosil matrix offers superior optical and mechanical properties, compared to polymer films, which have been previously reported for this type of sensor [34]. An ion-pairing technique was used to encapsulate the polar pH indicator in the non-polar ormosil matrix. Many reported optical CO_2 sensors are only sensitive up to $\sim 10\%$ CO_2 . To satisfy the requirements of the MAP application, the film developed here was tailored to respond over the full 0–100% CO_2 range. This was achieved by selecting the quaternary ammonium hydroxide base cetyltrimethylammonium hydroxide (CTA–OH) as the ion-pairing agent and internal buffer. This base also provided the water of crystallisation for the sensing chemistry. The amount of CTA–OH was adjusted to optimize the operational range. Calibration plots for this DLR sensor are shown in Fig. 9, illustrating the quality of the sensor performance achieved as well as the extended operational range. In the context of this paper, it is important to emphasize the advantages of adopting the sol-gel approach in developing this sensor film. Apart from the mechanical and optical properties of the film, the sol-gel approach facilitated the accommodation of relatively complex sensing chemistry. Moreover, the potential problem of oxygen cross-sensitivity in this sensor has been minimized by encapsulating the reference ruthenium complex in oxygen impermeable sol-gel

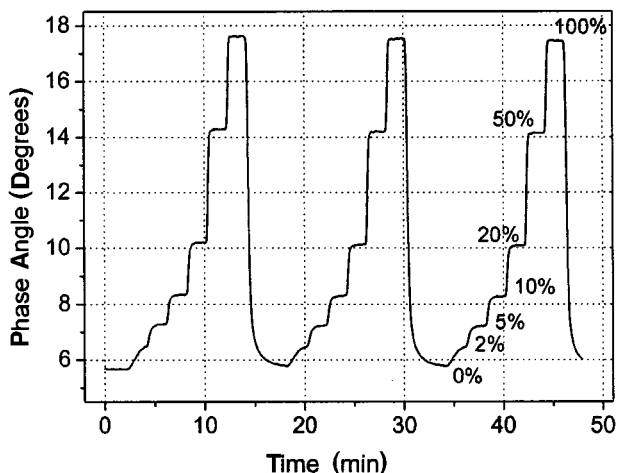


Fig. 9. Calibration plot for DLR-based CO₂ sensor.

microparticles, which are entirely compatible with the host matrix.

Sol-Gel Paint for Pressure Sensitive Paint (PSP) Applications

Conventionally, pressure measurements in aerodynamic testing are carried out by applying a series of individual pressure transducers (taps) across the surface of a model in a wind-tunnel. As the number of taps that can be applied is limited, these discrete pressure readings result in an incomplete pressure map. It is also a very expensive process.

More recently, pressure-sensitive paint (PSP) has been used in wind tunnel testing. This technique offers major advantages over current technology. The principle used is that oxygen in the airflow around the surface quenches the luminescence from an oxygen-sensitive dye in the paint, and by imaging the illuminated surface with a CCD camera, the oxygen profile, and hence the pressure profile of the surface, is mapped. PSP technology has the advantage of providing a continuous pressure distribution rather than measurements at a series of discrete pressure points. In addition, it is cheaper, non-invasive and relatively easy to prepare the model for testing. A new PSP system, which consists of a sol-gel MTEOS paint that is co-doped with an oxygen-sensitive ruthenium complex and a temperature-sensitive phosphor, manganese-activated magnesium fluorogermanate (MFG), has been developed [7]. Temperature correction is a major problem in PSP systems, and the strategy developed here is to co-dope an oxygen luminophore and a chemically inert temperature-dependent phosphor. These dopants have similar absorption bands, thereby facilitating the use of

a single excitation source, and fluorescent lifetimes that differ by orders of magnitude. This latter feature facilitates detection in the time domain with a single camera. Polymer binders have been used almost exclusively in PSP formulations. Some authors have used separate binders for the oxygen-sensitive luminophore and for the temperature phosphor. In the system reported here, a single porous sol-gel paint is used. There are a number of inherent advantages in choosing a sol-gel-based paint. As discussed previously, the process facilitates control over the film composition and porosity and, in particular for this application, the process allows fabrication of large area, homogeneous films at low cost. Spray coating was found to be the most effective coating method for this application while also ensuring that the fine MFG phosphor particles remained in suspension to produce a homogeneous distribution in the paint. The paint can be cured either at room temperature or at a slightly higher temperature (70°C) for a shorter period to give a porous, highly oxygen-sensitive matrix. The key features of this system are the use of a single excitation source and single camera, as well as the development of the dual-luminophore sol-gel paint. Preliminary calibration data has been obtained, and work is in progress to optimize the system to enable temperature-corrected pressure profiles of model surfaces in wind-tunnel conditions.

CONCLUSION

The versatility of the sol-gel process with regard to the design of optimized films for fluorescence-based sensing has been discussed in some detail. General principles of sensor optimization were presented. These included important issues such as immobilization efficiency, refractive index control and sensitivity enhancement. The advantages conferred by the use of ormosils and the contributions made by tailored sol-gel films in specific fluorescence-based sensor applications were emphasized. Although it has been clearly established that sol-gel-derived materials offer many advantages for sensor development, some key challenges remain to be overcome. Principal among these is the issue of long term stability of sensing films and the consequent impact on calibration function. To date, there has been no published demonstration of stable sensor performance over a period of 1 year or longer when using sol-gel films. This should be the major goal of future work in this area.

REFERENCES

1. B. Valeur (2002) *Molecular Fluorescence: Principles and Applications*, Wiley-VCH, Weinheim.

2. R. Zusman, C. Rottman, M. Ottolenghi, and D. Avnir (1990) "Doped sol-gel glasses as chemical sensors", *J. Non-Cryst. Solids* **122**, 107.
3. B. D. MacCraith (1997) "Optical chemical sensors based on sol-gel-derived films", in *Sol-Gel and Polymer Photonic Devices*, M. P. Andrews and S. I. Najafi (Eds.), SPIE, Bellingham, Washington.
4. C. J. Brinker and G. W. Scherer (1990) *Sol-Gel Science*, Academic Press, New York.
5. C. McDonagh, F. Sheridan, T. Butler, and B. D. MacCraith (1996) "Characterisation of sol-gel-derived silica films", *J. Non-Cryst. Solids* **194**, 72.
6. R. M. Almeida, X. Orignac, and D. Barbier (1994) "Silica-based sol-gel films doped with active elements", *J. Sol-gel Sci. Technol.* **2**, 1–3, 465.
7. J. Hradil, C. Davis, K. Mongey, C. McDonagh, and B. D. MacCraith (2002) "Temperature corrected pressure sensitive paint measurements using a single camera and a dual lifetime approach," accepted for publication in *Meas. Sci. Technol.*
8. A. Atkinson, J. Doorbar, A. Hudd, D. L. Segal, and P. J. White (1997) "Continuous Ink Jet Printing using Sol-gel Ceramic Links", *J. Sol-gel Sci. Technol.* **8**, 1093.
9. A. Bromberg, J. Zilberstein, S. Reisinger, E. Benori, W. Silberstein, J. Zimnavoda, G. Frishman, and A. Kritzman (1996) "Optical fibre sensors for blood gases and pH, based on porous glass tips", *Sensors Actuators B* **31**, 181.
10. C. Malins, S. Fanni, H. Glever, J. Vos, and B. D. MacCraith (1999) "The preparation of a sol-gel glass oxygen sensor incorporating a covalently bound fluorescent dye", *Anal. Commun.* **36**, 3–4, 3.
11. C. McDonagh, P. Bowe, K. Mongey, and B. D. MacCraith (2002) "Characterisation of porosity and sensor response times of sol-gel-derived thin films for oxygen sensor applications", *J. Non-Cryst. Solids* **306**, 2, 138–148.
12. C. McDonagh, B. D. MacCraith, and A. K. McEvoy (1998) "Tailoring of sol-gel films for optical sensing of oxygen in gas and aqueous phase", *Anal. Chem.* **70**, 45.
13. T. M. Butler, B. D. MacCraith, and C. McDonagh, (1998), "Leaching in sol-gel-derived silica films for optical pH sensors", *J. Non-Cryst. Solids* **224**, 249.
14. A. K. McEvoy, C. McDonagh, and B. D. MacCraith (1996) "Dissolved oxygen sensor based on fluorescence quenching of oxygen sensitive ruthenium complexes immobilised in sol-gel-derived porous silica coatings", *Analyst* **121**, 785.
15. K. Matsui, M. Tominaga, Y. Arai, H. Satoh, and M. Kyoto (1994) Fluorescence of pyrene in sol-gel silica derived from triethoxysilane, *J. Non-Cryst. Solids* **169**, 295.
16. P. Innocenzi, M. O. Abdirashid, and M. Guglielmi (1994) "Structure and properties of sol-gel coatings from methyltriethoxysilane and tetraethoxysilane", *J. Sol-gel Sci. Technol.* **3**, 47.
17. A. Mills (1998) "Controlling the sensitivity of optical oxygen sensors", *Sensors Actuators B* **51**, 60.
18. Y. Rharbi, A. Yekta, and M. A. Winnik (1999) "A method for measuring oxygen diffusion and oxygen permeation in polymer films based on fluorescence quenching", *Anal. Chem.* **71**, 5045.
19. E. R. Carraway, J. N. Demas, B. A. DeGraff, J. R. Bacon (1991) "Photophysics and photochemistry of oxygen sensors based on luminescent transition metal complexes", *Anal. Chem.* **63**, 337.
20. I. Klimant, F. Ruckruh, G. Liebsch, A. Stangelmayer, and O. S. Wolfbeis (1999) "Fast response oxygen micro-optodes based on novel ormosil glasses", *Mikrochim. Acta* **131**, 35.
21. A. Mills and Q. Chang (1992) "Modelled diffusion-controlled response and recovery behaviour of a naked optical film sensor with a hyperbolic-type response to analyte concentration", *Analyst* **117**, 1461.
22. H. Liu, S. C. Switalski, B. K. Coltrain, and P. B. Merkel (1992) "Oxygen permeability of sol-gel coatings", *Appl. Spec.* **46**, 1265.
23. A. E. Baron, J. D. S. Danielson, M. Gouterman, J. River Wan, J. B. Callis, and B. McLachlan (1993) "Submillisecond response times of oxygen-quenched luminescent coatings", *Rev. Sci. Instrum.* **64**, 3394.
24. B. D. MacCraith (1993) "Enhanced evanescent wave sensors based on sol-gel-derived porous glass coatings", *Sensors Actuators B* **11**, 29.
25. J. F. Gouin, A. Doyle, and B. D. MacCraith (1998) "Fluorescence capture by planar waveguide as platform for optical sensors", *Electronics Lett.* **34**, 1685.
26. L. Polerecky (2002) "Optimisation of multimode waveguide platforms for optical chemical sensors and biosensors," Ph. Thesis, unpublished.
27. G. Neurauter, I. Klimant, and O. S. Wolfbeis (1999) "Microsecond lifetime-based optical carbon dioxide sensor using luminescence resonance energy transfer", *Anal. Chim. Acta.* **382**, 67.
28. C. Huber, I. Klimant, C. Krause, T. Werner, T. Mayer, and O. S. Wolfbeis (2000) "Optical sensor for seawater salinity", *Fresenius J. Anal. Chem.* **368**, 196.
29. I. Klimant (1997) *German Pat. Appl.*, DE 198.29.657.
30. M. E. Lippitsch and S. Draxler (1993) "Luminescence decay-time-based optical sensors: principles and problems", *Sensors Actuators B* **11**, 97.
31. C. McDonagh, C. Kolle, A. K. McEvoy, D. L. Dowling, A. A. Cafolla, S. J. Cullen, and B. D. MacCraith (2001) "Phase fluorometric dissolved oxygen sensor", *Sensors Actuators B* **74**, 124.
32. C. Bultzingslowen, A. K. McEvoy, C. McDonagh, B. D. MacCraith, I. Klimant, C. Krause, and O. S. Wolfbeis (2002) "Sol-gel based optical carbon dioxide sensor employing dual luminophore referencing for application in food packaging technology", submitted to *The Analyst*.
33. I. Klimant, C. Huber, G. Liebsch, G. Neurauter, A. Strangelmayer, and O. S. Wolfbeis (2001) "Dual Lifetime Referencing (DLR): a new scheme for converting fluorescence intensity into a frequency-domain or time-domain information," in *Fluorescence Spectroscopy: New Methods and Applications*. B. Valeur and J. C. Maltoni (Eds.), Springer, Berlin.
34. B. G. McLachlan and J. H. Bell (1995) "Pressure-sensitive paint in aerodynamic testing", *Experimental Thermal Fluid Sci.* **10**, 470.
35. L. M. Coyle, D. Chapman, G. Khalil, E. Schibli, and M. Gouterman (1999) "Non-monotonic temperature dependence in molecular referenced pressure-sensitive paint (MR-PSP)", *J. Luminesc.* **82**, 33.
36. K. K. Gopinathan, R. Lakshminarayanan, N. Rajaram, M. I. A. Siddiq, and C. C. Suryanarayana (1977) "Magnesium Fluorogermanate red phosphor: temperature dependence of the emission spectrum", *Indian J. Phys.* **51B**, 423.
37. K. A. Wichersheim and M. H. Sun (1987) *Med. Electronics* **103**, 84.